Materials Horizons

Accepted Manuscript

This article can be cited before page numbers have been issued, to do this please use: J. Ge, X. Wang, H. Yao, H. Zhu, Y. Peng and S. Yu, *Mater. Horiz.*, 2015, DOI: 10.1039/C5MH00069F.

ROYAL SOCIETY OF CHEMISTRY

rsc.li/materials-horizons

Materials Horizons

Dynamic Article Links ►
View Article Online
DOI: 10.1039/C5MH00069F

Cite this: DOI: 10.1039/c0xx00000x

www.rsc.org/xxxxxx

ARTICLE TYPE

Durable Ag/AgCl nanowires assembled in sponge for continuous water purification under sunlight

Jin Ge‡,[a] Xu Wang‡,[a] Hong-Bin Yao,[a] Hong-Wu Zhu,[a] Yu-Can Peng,[a] Shu-Hong Yu*[a]

Received (in XXX, XXX) Xth XXXXXXXXX 20XX, Accepted Xth XXXXXXXXX 20XX
DOI: 10.1039/b000000x

Ag/AgCl nanowires (NW) sponge and a confined flow design were put forward to improve the photodegradation efficiency of immobilized Ag/AgCl NW catalysts. In consideration of the high cost of Ag/AgCl NW, an *in situ* recovery strategy was also provided to extend the lifetime of Ag/AgCl NW sponge.

Photocatalytic water purification by using sunlight as the energy source has been widely considered as a low-cost, environment friendly and sustainable technology for the decomposition of toxic organic pollutants into innocuous products (e.g., CO_2, H_2O).[1-3] One obstacle to its practical application is the inefficient use of visible-light which accounts 43% of the total sunlight. Silver halide are unstable under sunlight and have been used as photosensitive materials in the field of photographic films for many years. Recently, Wang et al.[4] found that after reducing some Ag^+ ions on the surface region of AgCl particles to Ag^0 species, the AgCl particles with silver nanoparticles formed on the surface exhibited ultra-high photocatalytic activity under visible-light. The degradation rate of the methyl orange (MO) over Ag/AgCl hybrid particles under visible-light irradiation was faster than that over N-doped TiO_2 by a factor of eight. This high performance is due to the surface plasmon resonance of silver nanoparticles which improves the absorption of visible light, and the enhanced separation of photogenerated electrons and holes at the metal-semiconductor interfaces.[5, 6] Beside the high photodegradation performance, the physicochemical structure of Ag/AgCl hybrid particles also exhibited high stability under UV and visible light, their photocatalytic activity experienced little change even after ten times of repeated usage. After this study, various Ag/AgCl based photocatalysts were fabricated and also showed high photodegradation efficiency to organic species under visible light.[7-17] Ag/AgCl based photocatalysts have been considered as promising materials for high speed water purification by using sunlight as the energy source due to their extremely high photodegradation efficiency to organic compound.

To promote the practical application of Ag/AgCl based photocatalysts in the industrial process, the complex and costly post-separation of these nanoscale particles from water should be solved.[1] The immobilization of Ag/AgCl nanostructures on the substrates of photoreactors is the most common approach to realize the instant separation of Ag/AgCl photocatalysts and water, and purify waste water in a continous mode. Directly mixing the Ag/AgCl nanostructures with binders and coating this mixture on the planner substrates of previously reported photoreactors[18-20] would resulted in 2D closely packed Ag/AgCl film with reduced active sites due to the contamination of the catalysts surface by binders and the low surface area of 2D planner substrates, which largely decreases the photoderadation speed per unit area of the photoreactor. In addition, the large diffusion distance of organic moliculars to the surface of Ag/AgCl film in the big reaction chambers of the photoreactors also reduce the photocatalytic water purification efficiency. Therefore, developing binder-free immobilization methods and novel photoreactors to improve the photocatalytic efficiency of immobilized Ag/AgCl nanostructures while having high throughput is highly in demand.

Herein, as showed in Scheme 1, we use polymer sponge as the substrate of photoreactor to imobilize Ag/AgCl nanowire (NW) networks (the resulted product named as PS@Ag/AgCl NW), forming robust three dimensional (3D) Ag/AgCl NW networks. To avoid losing the intrinsic high performance of Ag/AgCl NW, we developed a low temperature thermal welding method to immobilize intertwined Ag/AgCl NW networks on the backbones of the sponge. Compared to 2D Ag/AgCl hybrid film[21], 3D Ag/AgCl NW networks structure exposes more catalysts surface, and its unique open macropore system facilitate the passage of water flow and photons transfer to the catalysts surface. Furthermore, we fabricated a new photoreactor, in which the void space is completely occupied by the 3D Ag/AgCl NW networks, to confine the contaminated water only flowing through the irregular interconnected macropores. The confined flow in the photoreactor not only significantly decreased the diffusion distance of pollutants to Ag/AgCl NW surfaces from centimeters to micrometers, but also increased the probability of contact between pollutants and Ag/AgCl NW surfaces due to the enhanced fluid disturbance. The high photodegradation efficiency of 3D Ag/AgCl NW networks in the confined flow design was tested through photodegrading methyl orange (MO), and showed 4 times higher photodegradation efficiency than that of 2D Ag/AgCl film with a laminar gap. More importantly, the throughput of the photoreactor based on 3D Ag/AgCl NW networks with confined flow could reach up to 9600 L h^{-1} m^{-2}, which is two orders higher than that of microfluidic photoreactor (ca. 40 L h^{-1} m^{-2})[22]. We further developed a facile *in situ* chemical recovery method to extend the lifespan of Ag/AgCl NW on

View Article Online
DOI: 10.1039/C5MH00069F

backbones of sponge and thus reduce the material consumption. We anticipate that the 3D structuring of Ag/AgCl NWs, photoreactor with confined water flow design and *in situ* recovery strategy will promote the practical application of Ag/AgCl nanostructures for high speed, low cost and solar-powered water purification.

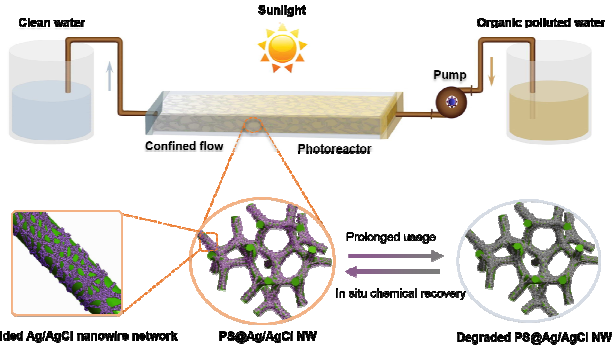

Scheme 1. Schematic illustration of a photoreactor based on welded Ag/AgCl hybrid nanowire (Ag/AgCl NW) coated sponge. Welded Ag/AgCl NW are tightly fixed on the backbone of a polymer sponge. The shell of the photoreactor wraps the Ag/AgCl NW coated sponge (PS@Ag/AgCl NW) with no gap leaved. During the usage of PS@Ag/AgCl NW, its color will change from purple to grey due to the photoreduction of Ag^+ to Ag^0. And its photocatalytic activity will gradually decrease. But through an *in situ* chemical recovery treatment to reduced Ag^0 back to Ag^+, the degraded performance of PS@Ag/AgCl NW after prolonged usage can be recovered

The fabrication procedures of 3D Ag/AgCl nanowire networks with highly mechanical stability are illustrated in Fig. 1a. Briefly, a polymer sponge (PS, Supplementary Fig. S1) was firstly coated with silver nanowires (AgNW) through dipping and drying processes as previously reported methods.[23-25] Then the AgNW coated polymer sponge was heated at 180 °C for 30 min to obtain 3D AgNW networks with welded joints (named as PS@AgNW). By dipping the PS@AgNW into $FeCl_3$ solution, AgNW on the sponge was oxidized to AgCl nanowires. Finally, polymer sponge supported welded 3D Ag/AgCl NW networks (named as PS@Ag/AgCl NW, Fig. 1b) was obtained by a photo irradiation treatment to reduce partial AgCl to metallic Ag on the surface of AgCl nanowires. The X-ray powder diffraction (XRD, Supplementary Fig. S2) of the PS@Ag/AgCl NW product clearly shows that the cubic phase of AgCl (JCPDF file: 31-1238) coexists with cubic phase of Ag (JCPDF file: 65-2871). The microstructure comparison of PS, PS@AgNW, and PS@Ag/AgCl NW (Fig. 1c, d, and e respectively) indicate that 3D Ag/AgCl NW networks were formed on the microfiber surface of the sponge. The magnified SEM (Fig. 1f) shows that the AgNW on the backbone of sponge are welded together at the contact point after thermal treatment. The magnified SEM (Fig. 1g) also shows that the weld Ag/AgCl NW were intertwined together rather than weakly physical contact between the nanowires by direct dip-coating of Ag/AgCl NW on the polymer sponge (Supplementary Fig. S3).

The anti-peeling of Ag/AgCl NW on the polymer sponge under water rush was examined by a homemade apparatus (Supplementary Fig. S4). The results (Fig. 1h) show that the weight of welded Ag/AgCl NW on the sponge substrate experienced little change after 12 hours of water flow wash even at a high speed of 180 $m^3\ m^{-2}\ h^{-1}$, while non-welded Ag/AgCl NW on the sponge substrate only retained 63% of the original weight under the same condition, indicating that the weld treatment played an important role in the formation of mechanically stable 3D Ag/AgCl NW networks.

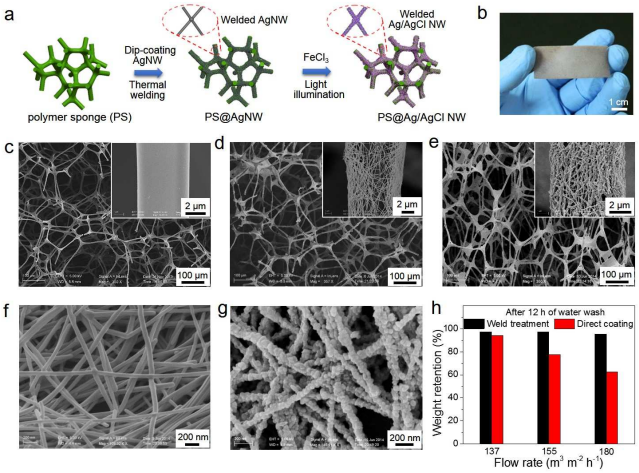

Fig. 1 (a) Schematic illustration of the fabrication processes of polymer sponge supported 3D Ag/AgCl NW networks (PS@Ag/AgCl NW). (b) A Photo of a typical sample of PS@Ag/AgCl NW. (c, d, e) SEM images of the origin polymer sponge, PS@AgNW and PS@Ag/AgCl NW, respectively. (f, g) High magnified SEM image of welded AgNW coating on the polymer sponge and welded Ag/AgCl NW coating on the polymer sponge, respectively. (h) The weight retention of 3D Ag/AgCl NW networks with welded joints and that with non-welded joints (direct coating method, Supplementary Fig. S3) after 12 h of water rush test at different water flow rate (volume of water per square sponge piece per hour).

Compared with laminar flow in the conventional photoreactors fixed with 2D thin film,[18, 19, 26-28] the water flow through the whole irregular 3D Ag/AgCl NW networks would greatly enhance the contact between reactants and the surfaces of Ag/AgCl NW. To the end, we made up a prototype photoreactor to confine the water flowing through the inner space of the 3D Ag/AgCl NW networks. As is illustrated in Fig. 2a, PS@Ag/AgCl NW was embedded into the middle cavity of the patterned silica rubber mat, then sandwiched between two Polymethyl methacrylate (PMMA) sheets (detailed methods see Supplementary Fig. S5). The advantage of this design is that the PS@Ag/AgCl NW closely contacts with the silicon rubber wall and organic glasses, leaving no gap except the macropores of PS@Ag/AgCl NW for water to flow through (Supplementary Fig. S5 c). Therefore, the micro sized pores (~300 um) serve as reaction chambers, which will efficiently shorten the diffusion distance of organic pollutants from water to the surfaces of Ag/AgCl NW. In addition, the interconnected tortuous macropores of the 3D Ag/AgCl NW networks act as static mixer and cause enhanced fluid disturbance, which greatly increase the probability of contact between organic pollutants and catalysts surfaces.

The advantages of 3D Ag/AgCl NW networks structure and confined flow design was demonstrated by photo bleaching methyl orange (MO) under a continuous-recirculation mode. As shown in Fig. 2c, a self-priming pump was used to feed the MO solution (30 mL, 8 mg/mL) to the photoreactor which was under visible light irradiation (300 W Xe arc lamp equipped with an UV-cutoff filter (≥420 nm), ca. 100 mW cm^{-2}) and circulate the outlet solution back to the MO reservoir. Meanwhile, the

View Article Online
DOI: 10.1039/C5MH00069F

performance of 2D Ag/AgCl NW film (Fig. 2c (i), Supplementary Fig. S6) and photoreactor based on the same 3D Ag/AgCl NW networks with a laminar gap (Fig. 2c (ii) were also tested under the same light irradiation, water flow rate and mass loading of catalyst, respectively. Fig. 2d clearly shows that the degradation efficiency of PS@Ag/AgCl NW based photoreactor with a laminar gap (Fig. 2c (ii)) is more than 2 times higher than that of Ag/AgCl NW film, demonstrating the advantage of 3D structured Ag/AgCl NW. However, the degradation efficiency of PS@Ag/AgCl NW with a laminar gap (Fig. 2c (ii)) is only half of that with confined flow design (Fig. 2c (iii)). This supports our design principle that confined flow induces close contact of MO moleculars and Ag/AgCl NW, leading to a higher photocatalytic efficiency. The mass transfer efficiency of 3D Ag/AgCl NW networks with confined flow can be further improved by increasing the flow rate which has great influence on the intensity of disturbance (Supplementary Fig. S7 a). The utilization of solar energy per unit area for the 3D Ag/AgCl NW networks can be maximized by increasing the mass loading of Ag/AgCl NW on per volume of polymer sponge and the thickness of PS@Ag/AgCl NW (Supplementary Fig. S 7b, c).

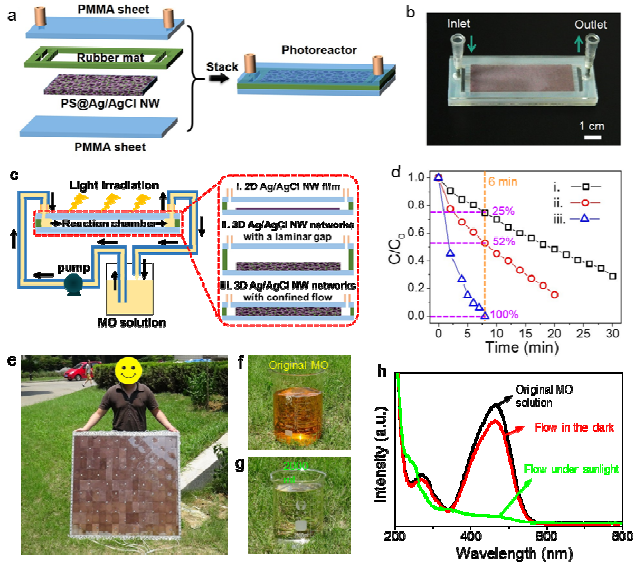

Fig. 2 (a) Fabrication of 3D Ag/AgCl NW nanowire networks based photoreactor with confined water flow. (b) Optical image of a photoreactor in which a typical PS@Ag/AgCl NW with 3 mm of thickness was fixed. (c) Schematic of the MO degradation test on three different photoreactor (i. Ag/AgCl NW film on a filter paper substrate (2 cm × 5 cm), the gap between top glass and the film is 2 mm; ii. the gap between top glass and PS@AgCl NW piece (2 cm × 5 cm × 3 mm) is 2 mm; iii. The same as ii expect no gap leaved). (d) MO degradation by the three different photoreactor versus time under the same light irradiation (300 W Xe arc lamp, 420 nm ~ 700 nm, 100 mW cm^{-2}), water flow rate (87.3 mL min^{-1}) and catalyst loading density (1.26 mg cm^{-2}). (e) Optical image of a polite modal photoreactor with one square meter large. (f, g) Optical image of origin MO solution (8 mg L^{-1}) and the degraded MO solution by the pilot-scale photoreactor under sunlight (42 mW cm^{-2}) at a flow rate of 1 L min^{-1}. (h) UV-Vis spectra of the original MO solution (black curve), 2 L of the MO solution flow through the pilot-scale photoreactor in the dark at a flow rate of 1 L min^{-1} (red curve), and the degraded MO solution mentioned in Fig. 3g (green curve).

To demonstrate the easily scalable fabrication and high performance of the 3D Ag/AgCl NW networks with confined flow under sunlight for practical application, a pilot-scale photoreactor with one square meter size was fabricated (Fig. 2e). The performance of this photoreactor was evaluated by bleaching MO in the real sunlight irradiation. Fig. 2f and 2g show that 2000 mL of yellow MO solution (8 mg L^{-1}) was completely bleached by the photoreactor in 2 min (Supplementary Movie S1). It should be noted that the absorption of MO moleculars on the PS@Ag/AgCl NW monolith contributes partially to concentration decrease of the MO solution. From the absorption spectra of the MO solution (2 L) that flowed through the photoreactor in the dark at a flow rate of 1 L min^{-1} (Fig. 2h), we can see that 14.6% of the MO molecules was absorbed by the PS@Ag/AgCl NW monolith.

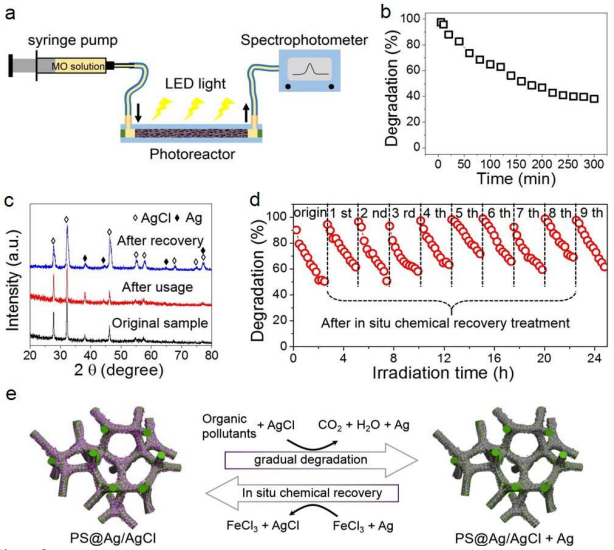

Fig. 3 (a) Schematic illustration of the stability evaluation system for PS@Ag/AgCl NW monolith. Commercial Light Emitting Diode (LED) light was chosen as the light source, for the LED light can continue working for more than 100 hours. The thickness of the PS@Ag/AgCl NW monolith is 1 mm, and the Ag/AgCl NW mass loading is 2.2 mg cm^{-3} (b) Change of MO degradation versus time for the original PS@Ag/AgCl NW monolith. (c) XRD patterns of the original, used and *in situ* recovered PS@Ag/AgCl NW monolith. (d) Degradation - *in situ* chemical recovery cycle test for PS@Ag/AgCl NW monolith. Each degradation cycle lasted for 2.5 h. (e) Schematic illustration of the *in situ* chemical recovery strategy used to extend the lifetime of PS@Ag/AgCl NW.

In addition to the high efficiency and high throughput of the photoreactor based on 3D Ag/AgCl NW networks with confined flow under visible light, the service time of the Ag/AgCl NW catalysts in the water treatment is also a key parameter. To evaluate the stability of 3D Ag/AgCl NW networks, long-time bleaching experiment for MO was performed. As illustrated in Fig. 3a, the MO solution was injected into the photoreactor by a syringe pump and degraded under white Light Emitting Diode (LED) lamp light irradiation (25 mW cm^{-2}). The residential time of MO in the photoreactor chamber was kept in 30 seconds. The MO concentration of the outlet solution was measured by UV-Vis spectrophotometer. Fig. 3b shows that the degradation efficiency of the PS@Ag/AgCl NW to MO gradually decreased to 42 % of its beginning value after 300 min of continuous operation. The XRD patterns of original and used PS@Ag/AgCl NW show that the relatively intensity of AgCl comparing to Ag decreased after the long-time operation (Fig. 3c), which indicates that the performance deterioration of PS@Ag/AgCl NW was caused by the gradual reduction of AgCl to elemental Ag during the photocatalytic process. This was further confirmed by the X-ray

View Article Online
DOI: 10.1039/C5MH00069F

photoelectron spectroscopy (XPS) of the origin and used PS@Ag/AgCl NW. From the XPS spectrum (Supplementary Fig. S8), the calculated surface mole ratio of the metallic Ag^0 to Ag^+ of origin PS@Ag/AgCl NW was 1 : 8.4. After 2.5 h of usage, the ratio of Ag^0 to Ag^+ increased to 1 : 4.1.

After understanding the inactivation mechanism, $FeCl_3$ solution was continuously pump through the photoreactor for 15 min to *in situ* oxide Ag back to AgCl. The XRD (Fig. 3c) and XPS (Supplementary Fig. S8) show that the AgCl was regenerated in the used PS@Ag/AgCl NW. The data in Fig. 3d demonstrates that the performance of the used PS@Ag/AgCl NW was recovered by the *in situ* chemical recovery processes. After repeating the degradation and recovery processes for nine times, the curve of degradation efficiency versus usage time almost kept the same as that of the original PS@Ag/AgCl NW. Therefore, even though the degradation efficiency of the PS@Ag/AgCl NW over MO reduced gradually during the photocatalytic processes due to the partial conversion of Ag^+ to Ag^0, the efficiency of PS@Ag/AgCl NW could be recovered by reducing Ag^0 back to Ag^+ through injecting $FeCl_3$ solution through the 3D Ag/AgCl NW networks for 15 min (Fig. 3e). And as a result, the PS@Ag/AgCl NW can be used for a long time while retaining high photodegradation efficiency.

Conclusions

In summary, we developed a welding method to fabricate robust 3D Ag/AgCl nanowires networks (Ag/AgCl NW) which exhibits higher photodegradation efficiency than 2D Ag/AgCl NW films, and proposed a new photoreactor with confined flow to further enhance the mass transfer efficiency of the 3D Ag/AgCl nanowires networks. This photoreactor with high throughput can be easily scaled up to one square meter large and exhibits high performance under sunlight. Furthermore, we demonstrated that the lifetime of the 3D Ag/AgCl nanowires networks can be largely prolonged by a facile *in situ* chemical recovery method. The 3D structuring of Ag/AgCl nanowire networks, combined with the confined flow design and *in situ* chemical recovery strategy, will pave the way for the practical application of Ag/AgCl nanostructures in solar-powered water purification with high efficiency and throughput in the future.

Acknowledgment

S.H.Y. acknowledges the funding support from the National Basic Research Program of China (Grants 2014CB931800, 2013CB933900), the National Natural Science Foundation of China (Grants 21431006, 91227103, 21061160492, J1030412), and the Chinese Academy of Sciences (Grant KJZD-EW-M01-1).

Notes and references

[a] *Division of Nanomaterials & Chemistry, Hefei National Laboratory for Physical Sciences at Microscale, Department of Chemistry, University of Science and Technology of China, Hefei, Anhui 230026, The People's Republic of China. Fax: +86 0551-63603040; E-mail: shyu@ustc.edu.cn.*

† Electronic Supplementary Information (ESI) available: [details of any supplementary information available should be included here]. See DOI: 10.1039/b000000x/

‡ These authors contributed equally to this work.

1 M. N. Chong, B. Jin, C. W. K. Chow and C. Saint, *Water Res.*, 2010, **44**, 2997.
2 C. Chen, W. Ma and J. Zhao, *Chem. Soc. Rev.*, 2010, **39**, 4206.
3 A. Kubacka, M. Fernandez-Garcia and G. Colon, *Chem. Rev.*, 2011, **112**, 1555.
4 P. Wang, B. Huang, X. Qin, X. Zhang, Y. Dai, J. Wei and M. H. Whangbo, *Angew. Chem. Int. Ed.*, 2008, **47**, 7931.
5 Z. Z. Lou, Z. Y. Wang, B. B. Huang and Y. Dai, *Chemcatchem*, 2014, **6**, 2456.
6 P. Wang, B. B. Huang, Y. Dai and M. H. Whangbo, *Phys. Chem. Chem. Phys.*, 2012, **14**, 9813.
7 C. H. An, S. N. Peng and Y. G. Sun, *Adv. Mater.*, 2010, **22**, 2570.
8 M. Choi, K. H. Shin and J. Jang, *J. Colloid Interface Sci.*, 2010, **341**, 83.
9 Y. Y. Li and Y. Ding, *J Phys. Chem. C*, 2010, **114**, 3175.
10 Y. G. Sun, *J Phys. Chem. C*, 2010, **114**, 2127.
11 L. Han, P. Wang, C. Z. Zhu, Y. M. Zhai and S. J. Dong, *Nanoscale*, 2011, **3**, 2931.
12 J. Jiang and L. Z. Zhang, *Chem. Eur. J*, 2011, **17**, 3710.
13 H. Xu, H. M. Li, J. X. Xia, S. Yin, Z. J. Luo, L. Liu and L. Xu, *Acs. Appl. Mater. Inter.*, 2011, **3**, 22.
14 H. Zhang, X. F. Fan, X. Quan, S. Chen and H. T. Yu, *Environ. Sci. Technol.*, 2011, **45**, 5731.
15 M. S. Zhu, P. L. Chen and M. H. Liu, *Acs Nano*, 2011, **5**, 4529.
16 J. H. Kou and R. S. Varma, *Chemsuschem*, 2012, **5**, 2435.
17 H. X. Shi, J. Y. Chen, G. Y. Li, X. Nie, H. J. Zhao, P. K. Wong and T. C. An, *Acs Appl. Mater. Inter.*, 2013, **5**, 6959.
18 J. Senthilnathan and L. Philip, *Solar Energy*, 2012, **86**, 2735.
19 G. Zayani, L. Bousselmi, F. Mhenni and A. Ghrabi, *Desalination*, 2009, **246**, 344.
20 N. M. Mahmoodi, M. Arami and N. Y. Limaee, *J. Hazard. Mater.*, 2006, **133**, 113.
21 L. Han, Z. K. Xu, P. Wang and S. J. Dong, *Chem. Commun.*, 2013, **49**, 4953.
22 L. Lei, N. Wang, X. M. Zhang, Q. D. Tai, D. P. Tsai and H. L. W. Chan, *Biomicrofluidics*, 2010, **4**,
23 J. Ge, Y.-D. Ye, H.-B. Yao, X. Zhu, X. Wang, L. Wu, J.-L. Wang, H. Ding, N. Yong, L.-H. He and S.-H. Yu, *Angew. Chem. Int. Ed.*, 2014, **53**, 3612.
24 J. Ge, H.-B. Yao, X. Wang, Y.-D. Ye, J.-L. Wang, Z.-Y. Wu, J.-W. Liu, F.-J. Fan, H.-L. Gao, C.-L. Zhang and S.-H. Yu, *Angew. Chem. Int. Ed.*, 2013, **52**, 1654.
25 H.-B. Yao, J. Ge, C.-F. Wang, X. Wang, W. Hu, Z.-J. Zheng, Y. Ni and S.-H. Yu, *Adv. Mater.*, 2013, **25**, 6692.
26 Y.-L. Kuo, T.-L. Su, K.-J. Chuang, H.-W. Chen and F.-C. Kung, *Environ. Technol.*, 2011, **32**, 1799.
27 X. Wang, X. Tan and T. Yu, *Ind. Eng. Chem. Res.*, 2014, **53**, 7902.
28 P.-J. Lu, C.-W. Chien, T.-S. Chen and J.-M. Chern, *Chem. Eng. J.*, 2010, **163**, 28.

View Article Online
DOI: 10.1039/C5MH00069F

Graphic Figure

The 3D structuring of Ag/AgCl nanowire, combined with the confined flow design greatly improve the photodegradation efficiency of Ag/AgCl nanostructures in immobilized form. The *in situ* recovery strategy also extend the lifetime of Ag/AgCl nanostructures.

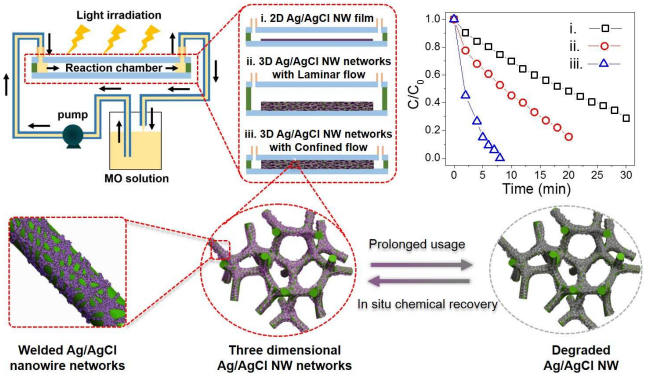

View Article Online
DOI: 10.1039/C5MH00069F

Conceptual Insights Statement

We for the first time fabricated robust 3D Ag/AgCl nanowire (NW) networks on a polymer sponge with interconnected macropores through a low temperature welding method. This binder free method avoids contaminating the surface of Ag/AgCl NW. Compared to 2D film, this 3D Ag/AgCl nanowire network exposes more catalysts surface and its unique open macropores system also benefits the fast diffusion of reactants to the catalysts surface.

We put forward a confined flow design for the photoreactor based on the above 3D Ag/AgCl NW network to shorten the diffusion distance of organic pollutants to the catalyst surface and at the same time enhance the mass transfer speed. This design improves the photodegradation efficiency for more than two times compared with conventional lamellar flow design. This photoreactor can be easily scale up to one square meter large. To our best knowledge, this is the first huge photoreactor immobilized with Ag/AgCl nanostructures so far.

Furthermore, our proposed in situ chemical recovery strategy, which can extend the lifetime of the immobilized Ag/AgCl NW and thus reduce the material consumption, makes the Ag/AgCl NW based photoreactor less cost efficient and more competitive.